A new approach to the dynamics of hydrogen bond network in liquid water

Masakazu Matsumoto[a)]
Department of Structural Molecular Science, The Graduate University for Advanced Studies, Myodaiji, Okazaki, 444 Japan

Iwao Ohmine
Department of Chemistry, Faculty of Science, Nagoya University, Furo-cho, Chikusa-ku, Nagoya, 464-01 Japan

(Received 16 August 1995; accepted 9 November 1995)

The relation between topology and rearrangement dynamics of the hydrogen bond network (HBN) in the supercooled liquid water is investigated by using molecular dynamics (MD) calculation and examining topological indices. We have found that there is very strong correlation among certain pairs of hydrogen bonds. HBN is shown to be represented by an ''undirected'' graph. Topology and rearrangement dynamics of HBN are then simply described in terms of the network defects and their motions. Based on this fact, a new lattice dynamic model is proposed. The model shows that spontaneous heterogeneous hydrogen bond rearrangement occurs even when the network structure is homogeneous. © *1996 American Institute of Physics.* [S0021-9606(96)50507-6]

I. INTRODUCTION

Molecular dynamics in liquid water is intermittent and collective, yielding large energy fluctuation.[1–3] To understand such molecular motions, the detailed knowledge of temporal and spatial correlations of hydrogen bonds is required. There have been many attempts to clarify the origin of the collective dynamics in water by using normal mode analysis, the instantaneous normal mode analysis, many kinds of lattice models and others.[1,4–7]

Many static and dynamic properties of water have been characterized in terms of hydrogen bond network (HBN) structure and its rearrangement. Numerous attempts have been made to show the relationship between ''topology'' of the HBN and its ''dynamics.'' Stanley *et al.* first introduced the idea of percolation into HBN, and succeeded to explain many static and macroscopic dynamical anomalies of water.[5,8] Our understanding of water behavior is, however, far from complete. Even the location of spinodal lines is not fully determined yet.[6,9–15] Recently the second critical point and idea of water II phase have been proposed and the situation becomes even more (interesting but) complicated.[16–18]

In the present work we investigate the dynamical properties of water in the supercooled regime. Our knowledge of the supercooled water dynamics is still limited. Stanley *et al.* proposed the role of the water with 5 coordination,[19,20] where they emphasized the correlation between z (coordination number) and local diffusion coefficient. Stillinger attempted to impose icelike structure into polyhedron,[21] while Speedy attempted to find it in HB ring structure.[22] Sasai showed that the hydrogen bond rearrangement is collective.[6] However, the detailed correlation among the structural parameters and the dynamics of water molecules has not been examined yet. In this paper, we extract the kernel of the heterogeneous hydrogen bond rearrangement and clarify how the structure and the dynamics are related.

Molecular dynamics method used in the simulation is briefly described in Sec. II. Topological parameters characterizing the hydrogen bond rearrangement (HBR) are introduced and their mutual correlations are examined in Sec. III. In Sec. IV, the graph theory is utilized to understand the dynamics of HBN and the new definition of the network defects is proposed. In Sec. V, a new dynamical lattice model is proposed to describe the hydrogen bond network rearrangement dynamics in the supercooled water. Conclusions are given in Sec. VI.

II. MOLECULAR DYNAMICS SIMULATION

In order to determine important topological indices expressing the hydrogen bond rearrangement dynamics, we have performed the molecular dynamics (MD) calculations for the supercooled water systems. The simulation is performed for the system with 216 water molecules contained in a cubic box. A periodic boundary condition is applied. Andersen's constant-pressure method[23] and Nose's constant-temperature method[24] are implemented in the MD calculations. Pressure is kept in atmospheric value. Several temperatures between 300 K and 200 K are arbitrarily chosen. TIP4P potential function[25] is used and long-ranged intermolecular interaction is truncated with a smooth function around 9 Å . Trajectories are recorded for about 100 to 1000 ps, depending on temperature.

Although there are many ways to define the HB (hydrogen bonds), we here use the simplest definition; two water molecules are hydrogen bonded if their interaction energy is lower than -10 kJ/mol. HB is formed between the nearest hydrogen and oxygen pair of these molecules.

[a)]Current address: Department of Chemistry, Faculty of Science, Nagoya University, Furo-cho, Chikusa-ku, Nagoya, 464-01 Japan. E-mail address: matto@aqua.chem.nagoya-u.ac.jp

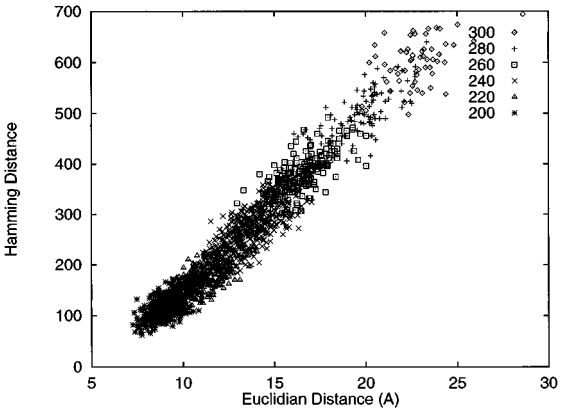

FIG. 1. Hamming distance is plotted against Euclidean distance. They are calculated from successive MD configurations in 1 ps interval.

III. TOPOLOGICAL AND DYNAMIC PARAMETERS

To find molecular motions in liquid, the ''distance'' between two configurations at different times is a very useful measure. Euclidean distance is defined by

$$D(t,t')=\left(\sum_{i=1}^{N}|\mathbf{r}_i(t)-\mathbf{r}_i(t')|^2\right)^{1/2}, \tag{1}$$

where $\mathbf{r}_i(t)$ is the position of the center of mass of ith water molecule at time t. In the previous work,[1] we have shown how the collective motions are seen in the distance matrices. It is of interest to understand how the distance is related to the changes of HBN. The instantaneous topology of the HBN in the system with N water molecules can be expressed as the binary $N\times N$ symmetric connection matrix, where each element $\{i,j\}$ gives 1 if molecule i is binded with molecule j and 0 otherwise. Then the ''Hamming distance,'' a term from information theory, can be defined as the number of different elements between two matrices. The correlation between Hamming distance and Euclidean distance of the two successive structures is plotted in Fig. 1. We can see in the figure that the change in HBN linearly corresponds to translation of the molecules over all temperature range.

In order to analyze the HBN rearrangement, topological indices of the network should be defined. They might be ''rings''[22] or ''polyhedra''[21] of the HBN. However, these indices defined with more than two molecules are difficult to trace and may cause ambiguity. We thus choose only unimolecular topological indices, as the structural indices. Examples are listed in Table I. We here use a mark, a right arrow ($\rightarrow$), to indicate a donating (i.e., ''outgoing'') hydrogen bond of the specified water molecule, a hydrogen of the water molecule making HB with the oxygen of another water molecule. A left arrow ($\leftarrow$) to indicate an accepting (i.e., ''incoming'') hydrogen bond, the oxygen of the water molecule making HB with a hydrogen of another water molecule. We also choose the local indices of dynamics in Table II. Each index $\Delta x(t)$ is defined as $\Delta x(t)=x(t+\Delta t)-x(t)$, except $\tilde{D}$. They depend strongly upon the choice of Δt; we choose 1 ps and 100 fs for Δt.

TABLE I. Various topological indices. Some of them are not utilized or not mentioned in this paper.

z_A	Number of adjacent molecules,defined as the number of molecules nearer than $r_C=3.5$ Å
z_{HB}	Number of HBs of a molecule
$\overleftarrow{z}_{HB},\vec{z}_{HB}$	Number of the accepting / donating HBs
z_V	Number of adjacent molecules, defined as the number of faces of Voronoi polyhedron
V_V	Volume of Voronoi polyhedron
S_V	Surface area of Voronoi polyhedron
z'_{HB}	Number of weak HBs, having the HB energies between -10 and -5 kJ/mol
E_B	Binding energy

To evaluate the magnitude of correlation, we use two standards. First, the simultaneous correlation coefficient between a time sequence of a variable $\{x(t_1),\ldots,x(t_i),\ldots,x(t_N)\}$ and another $\{y(t_1),\ldots,y(t_i),\ldots,y(t_N)\}$ is defined by

$$C(\{x\},\{y\})=\frac{(1/N)\Sigma x(t_i)\cdot y(t_i)}{[(1/N)\Sigma x(t_i)][(1/N)\Sigma y(t_i))}=\frac{\langle x\cdot y\rangle}{\langle x\rangle\langle y\rangle}. \tag{2}$$

This coefficient indicates the strength of linear correlation between two sequences and has a value between -1 to 1.

If the two sequences correlate nonlinearly, another type of correlation should be used. We here utilize the mutual information $I(\{x\}:\{y\})$. The probability of taking the value x_i can be denoted as $P(x_i)$. The information of the data set is defined as

$$H(\{x\})=-\sum_i P(x_i)\log P(x_i). \tag{3}$$

The information $H(\{y\})$ can also be defined for another sequential data set $\{y\}$. The joint probability $P(x_i,y_j)$ is the probability that x is x_i and y is y_j at the same time. Its information is calculated in the same manner as follows:

$$H(\{x\},\{y\})=-\sum_{ij} P(x_i,y_j)\log P(x_i,y_j). \tag{4}$$

Then the mutual information is defined as

TABLE II. Various indices of structure rearrangement.

$\tilde{D}$	Local diffusion coefficient calculated from the displacement between 1 to 2 ps after the moment Ref. 26
Δr^2	Square displacement of the center of mass just after the moment
$\Delta\theta$	Rotation angle just after the moment
Δz_{HB}	Change of the number of HBs
$\Delta\vec{z}_{HB}$	Change of the number of the donating HBs
$\Delta\overleftarrow{z}_{HB}$	Change of the number of the accepting HBs
$\Delta\vec{z}^{+}_{HB}$	Increment of the number of the donating HBs
$\Delta\overleftarrow{z}^{+}_{HB}$	Increment of the number of the accepting HBs
$\Delta\vec{z}^{-}_{HB}$	Decrement of the number of the donating HBs
$\Delta\overleftarrow{z}^{-}_{HB}$	Decrement of the number of the accepting HBs

TABLE III. Various correlation between two topological index at 240 K. Upper: correlation coefficient. Lower: mutual information. H is a single information.

H	H	z_A 1.1319	z_{HB} 0.996	$\vec{z}_{HB}$ 5.74	$\overleftarrow{z}_{HB}$ 0.740	E_B
z_A			0.0543	0.0158	0.0722	0.0974
	1.319		0.0533	0.0198	0.0494	
z_{HB}				0.6459	0.7616	−0.3378
	0.996			0.2365	0.4014	
$\vec{z}_{HB}$					0.0397	−0.1558
	0.574				0.0015	
$\overleftarrow{z}_{HB}$						−0.3278
	0.740					

$$I(\{x\}:\{y\})=H(\{x\})+H(\{y\})-H(\{x\},\{y\}), \tag{5}$$

which indicates the excess information produced by the correlation of two sets. It becomes 0 if there is no correlation between x and y. As there is any averaging operation in the definition, this index is applicable even when x does not take ordered value. Mutual information is not utilized for continuous topological indices in this work. Although there are various ways to take the time correlation, for examples, delayed correlations, correlations between distant points and many body correlations, we take only simultaneous correlations in this work.

Let us now look at these correlations in detail. The correlations among topological indices are listed in Table III. The correlation between $\overleftarrow{z}_{HB}$ (the number of the accepting HBs) and $\vec{z}_{HB}$ (the number of the donating HBs) is strikingly small $[C(\overleftarrow{z}_{HB},\vec{z}_{HB})=0.0397]$; the number of incoming HBs does not correlate with the number of outgoing HBs.

Relatively large negative correlation between z_{HB} and E_B simply indicates the fact that the more HBs a water molecule has, the lower its binding energy becomes.

Table IV shows the relation between topological index and its change. There are strong correlations between $[\vec{z}_{HB},\Delta\vec{z}^{+}_{HB}$(increment of the number of the donating HBs)], $[\vec{z}_{HB},\Delta\vec{z}^{-}_{HB}$(decrement of the number of donating HBs)], $[\overleftarrow{z}_{HB},\Delta\overleftarrow{z}^{+}_{HB}$(increment of the number of the accepting HBs)], $[\overleftarrow{z}_{HB},\Delta\overleftarrow{z}^{-}_{HB}$(decrement of the number of the accepting HBs)]. On the other hand, $\vec{z}_{HB}$ yields small correlation with $\Delta\overleftarrow{z}^{+}_{HB}$ and with $\Delta\overleftarrow{z}^{-}_{HB}$ The negative large correlation between $\Delta\theta$ (rotation angle) and z_{HB} simply implies that water molecule can rotate easily when the number of HBs is small.

The relation between two indices of structural change is also interesting. Table V shows that the decrement of the number of outgoing HBs strongly causes the simultaneous increment of the number of outgoing HBs, $C(\Delta\vec{z}^{+}_{HB},\Delta\vec{z}^{-}_{HB})=0.5169$, and so that the number of outgoing HBs does not much change from 2 even when bond alternations take place. There is also significant correlation between increment and decrement of the number of incoming HBs $C(\Delta\overleftarrow{z}^{+}_{HB},\Delta\overleftarrow{z}^{-}_{HB})=0.2689$, which is but less than $C(\Delta\vec{z}^{+}_{HB},\Delta\vec{z}^{-}_{HB})=0.5169$ because three incoming hydrogen bonds per a water molecule is possible. On the other hand, there is only small correlation between simultaneous change of the number of incoming and outgoing HBs $[C(\Delta\vec{z}^{+}_{HB},\Delta\overleftarrow{z}^{+}_{HB})=0.0948$, $C(\Delta\vec{z}^{+}_{HB},\Delta\overleftarrow{z}^{-}_{HB})=0.0663$, $C(\Delta\vec{z}^{-}_{HB},\Delta\overleftarrow{z}^{+}_{HB})=0.0632$, $C(\Delta\vec{z}^{-}_{HB},\Delta\overleftarrow{z}^{-}_{HB})=0.0989]$. The large correlations with Δr^2 (square displacement of the center of mass) or $\Delta\theta$ shows that any kind of HBR causes translation or rotation of the molecule.

TABLE IV. Various correlation between topological index and dynamic index at 240 K. Δt is 100 fs. Upper: correlation coefficient. Lower: mutual information. H is a single information.

H	H	z_A 1.346	z_{HB} 1.022	$\vec{z}_{HB}$ 0.589	$\overleftarrow{z}_{HB}$ 0.765	E_B
$\Delta\vec{z}_{HB}$		0.1660	−0.2154	−0.2995	−0.0479	0.2712
	0.765	0.0152	0.0454	0.1190	0.0013	
$\Delta\overleftarrow{z}_{HB}$		0.1773	−0.0859	0.0041	−0.1272	0.0575
	0.754	0.0164	0.0313	0.0002	0.0607	
$\Delta\vec{z}^{+}_{HB}$		0.1033	−0.4082	−0.6353	−0.0291	0.2024
	0.488	0.0070	0.0853	0.1802	0.0005	
$\Delta\overleftarrow{z}^{+}_{HB}$		0.1050	−0.3352	0.0152	−0.4730	0.0417
	0.487	0.0060	0.0612	0.0002	0.1131	
$\Delta\vec{z}^{-}_{HB}$		0.1445	0.0876	0.1897	−0.0424	0.2024
	0.487	0.0105	0.0068	0.0348	0.0009	
$\Delta\overleftarrow{z}^{-}_{HB}$		0.1482	0.2137	−0.0094	0.2929	0.0404
	0.486	0.0117	0.0305	0.0001	0.0502	
Δr^2		0.0262	−0.0915	−0.0589	−0.0779	0.1580
$\Delta\theta$		0.0729	−0.5703	−0.2908	−0.5228	0.2957

There is a certain relation between the average square displacement $\overline{\Delta r^2}$ and the coordination number z_A.[26,19] However, the direct correlation between the square displacement before averaged, Δr^2, and the coordination number, z_A, is very small $[C(z_A,\Delta r^2)=-0.0659$ for $\Delta t=1$ ps, 0.0262 for $\Delta t=100$ fs]. This is because the distribution of Δr^2 is very broad. Δr^2 is an inadequate index to perform the correlation analysis.

As a summary, the MD calculation reveals that

—Four HBs are not equivalent.

—The number of incoming and outgoing HBs are independently controlled to be around 2. As the result, total number of HBs per a water molecule becomes to about 4.

IV. GRAPHICAL ANALYSIS

In this section, we propose a new graphical representation of the hydrogen bond network, which leads naturally to a new concept of defects. Correlated motion of the hydrogen bonds is then described in terms of the network topology and defect.

The topology of the HBN of water can be represented by a graph, where nodes and bonds correspond to water molecules and hydrogen bonds, respectively. In the liquid water, there are several water molecules surrounding an individual water molecule, but not making HBs with that central water molecule. These surrounding water molecules easily turn to

TABLE V. Various correlation between two dynamic index at 240 K. Δt is 1 ps. Upper: correlation coefficient. Lower: mutual information. H is a single information.

H	H	$\Delta\vec{z}_{HB}$ 0.765	$\Delta\overleftarrow{z}_{HB}$ 0.789	$\Delta\vec{z}^{+}_{HB}$ 0.504	$\Delta\overleftarrow{z}^{+}_{HB}$ 0.499	$\Delta\vec{z}^{-}_{HB}$ 0.504	$\Delta\overleftarrow{z}^{-}_{HB}$ 0.499	Δr^2	$\Delta\theta$
$\Delta\vec{z}_{HB}$			0.1165	0.8706	0.0907	0.8712	0.0949	0.3459	0.5199
	0.765		0.0077	0.3734	0.0043	0.3735	0.0045		
$\Delta\overleftarrow{z}_{HB}$				0.1011	0.7965	0.1018	0.7965	0.3764	0.3600
	0.789			0.0053	0.3206	0.0055	0.3204		
$\Delta\vec{z}^{+}_{HB}$					0.0948	0.5169	0.0663	0.3052	0.4536
	0.504				0.0041	0.1118	0.0021		
$\Delta\overleftarrow{z}^{+}_{HB}$						0.0632	0.2689	0.2953	0.2839
	0.499					0.0019	0.0304		
$\Delta\vec{z}^{-}_{HB}$							0.0989	0.2972	0.4518
	0.504						0.0045		
$\Delta\overleftarrow{z}^{-}_{HB}$								0.3043	0.2896
	0.499								
Δr^2									0.5212

make HBs with the central water molecule. We introduce here the ''virtual HB'' to represent the non-HB bond between the adjacent water molecules, which is ready to change to HB. The new topological graph of the network, constructed with HBs and virtual HBs is able to describe the geometrical information for possible HB alternations, thus can treat the HB rearrangement dynamics. We use the term ''adjacency bonds'' to indicate both real and virtual bonds.

Let us consider graphical representation of HBN. The HBN, indicated in Fig. 3(a), can simply be represented by a directed graph, shown in Fig 3(b). Each node and arrow corresponds to the water molecule and HB, respectively. Here, an incoming arrow to a node indicates that a hydrogen of another water molecule makes a HB with the oxygen of that node (water molecule). An outgoing arrow from a node, a water molecule, indicates that a hydrogen of that node (water molecule) makes a HB with an oxygen of another water molecule. Dashed bonds are added to denote the virtual HBs. Each node nearly has two incoming and two outgoing HBs. Each arrow is further replaced by a bond with white and black circles at the head and the tail of the arrow, respectively. The diagram of HBN obtained after this operation is shown in Fig. 3(c). As we have seen in the previous section, the events of incoming bonds are nearly independent from the events of outgoing bonds; the white circles and the black circles are not mutually exchangeable. White circles in a node can then be put together into one white circle and black ones to one black one, as shown in Fig. 3(d). Each node is separated into two vertices; one for a donating part of the node (black circle) and the other for an accepting part (white circle). The bonds are then no longer necessarily to be represented with directed allows. By this operation, HBN is converted into an undirected infinite graph. The number of vertices is twice of that of nodes and thus the number of edges at each vertex becomes half. Here, we use the notations of ''vertex'' and ''edge'' in the undirected graph whereas we have used ''node'' and ''bond'' in the directed graph, respectively.

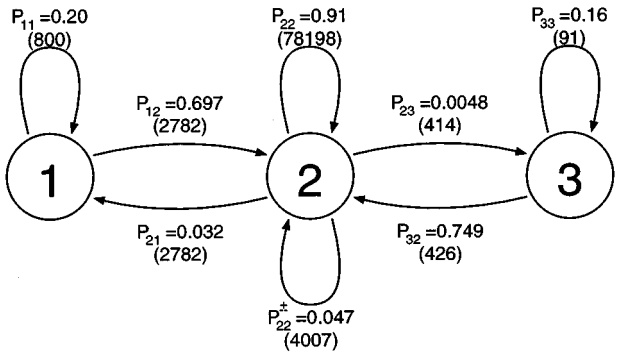

FIG. 2. State transition diagram of a node at 220 K, extracted from the MD data. The state (i) of the node is specified by the number (i) of the donating HBs from that node. P_{ij} denotes the transition probability from state i to state j. $P^{\pm}_{22}$ is the probability that one HB is detached and another is connected at a same time. The number in parentheses are raw occurrence number in the simulation. Δt is 1 ps.

Each edge is either of ''occupied'' or ''vacant'' state. An occupied edge is called a ''hydrogen edge (HE).'' A vacant edge is an virtual HE. Each vertex is assumed to have not less than two virtual HEs. We assume that the number of HEs attached to one vertex takes the value between 1 to 3. This is a reasonable assumption because water molecules having 0 or 4 incoming / outgoing HEs are quite rare in the real water. We draw the state transition among HB states at a node using the MD data in the previous section. Figure 2 shows the changes of HBs at 220 K. Each arrow denotes the transition probabilities to various HB states in a step. Infrequent transitions are omitted from the diagram. The large probability P_{12} and P_{32} indicates that water molecule with 1 or 3 donating HB will change to have two donating HB quickly. The lower loop $P^{\pm}_{22}$ denotes that one of the two HBs is diminished and another HB is created at a time. The most probable total number of the donating HBs is thus two. The same is true for the accepting HBs.

We define the vertex with more or less than two HEs as defect. There are oversatisfied (having more than two HEs; denoted by $\oplus$) and dissatisfied (less than two HEs; $\ominus$) types of defects. A state transition of an edge always causes one of

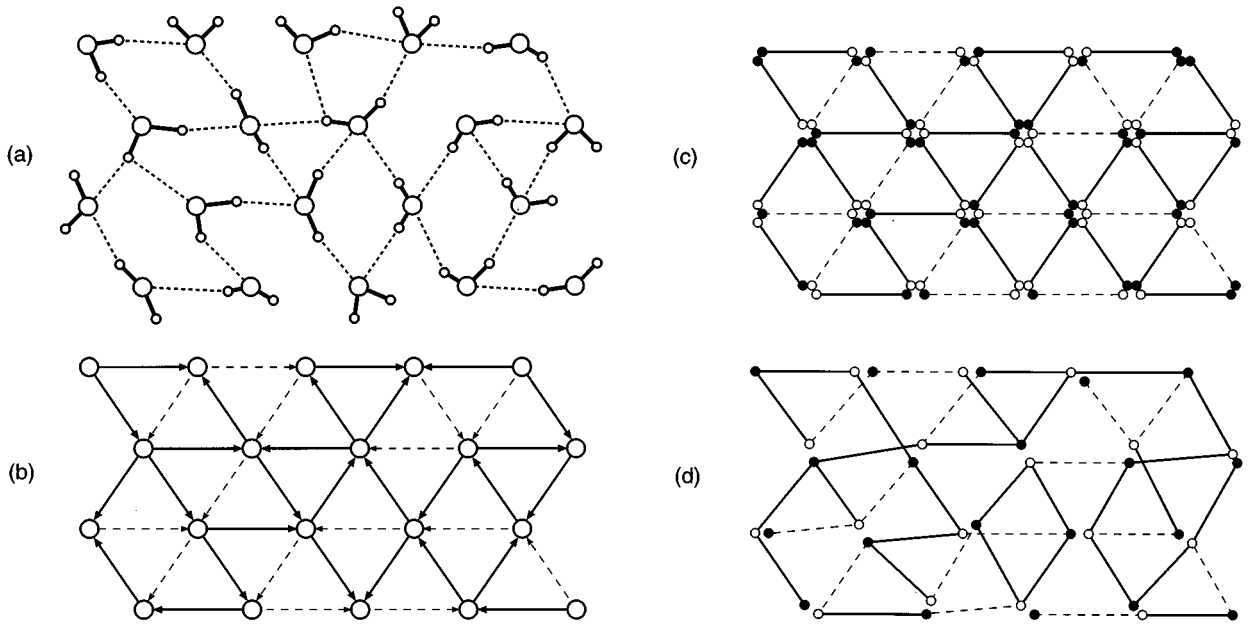

FIG. 3. Separation scheme of the HB network. (a) The original HBN in liquid water; (b) the same network represented by digraph (i.e., directed graph). Virtual HBs are added; (c) arrows are replaced by the bond with black and white circles; (d) black (white) circles are gathered and the network reduces to an undirected graph.

the three types of the defect motion, propagation, pair creation and pair annihilation, as illustrated in Fig. 4.

A HB annihilation probability is enumerated by the number of HBs attached to each vertex. When both vertices are $\oplus$ defects, the HB (and thus both defects) annihilates with a probability, say, p. When one end is $\oplus$ defect, the HB annihilates with a probability q and the other end becomes $\ominus$ defect. While both ends are not $\oplus$ defects, the HB annihilates with a low probability r. p, q and r should be called as ''pair annihilation probability,'' ''propagation probability'' and ''pair creation probability,'' respectively. In Table VI, p, q and r extracted from MD data are 0.72, 0.29, and 0.10, respectively.

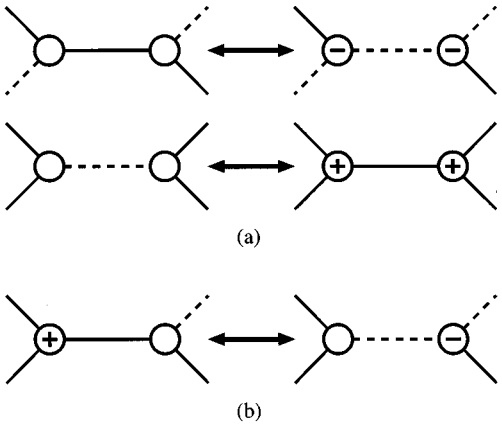

FIG. 4. Three types of defect motion. (a) Creation and annihilation of defect pair; (b) propagation of a defect. Dashed line denotes the virtual HE and solid line the HE. + and − indicate the oversatisfied and dissatisfied types of the defect, respectively.

It is important to know the defect dynamics that once a defect is created, it can never cease until it reaches a partner defect to annihilate with. This situation is very close to so called ''domino phenomenon;'' once one defect passes over a path, another defect never can pass the same path and defect stops when it meets another defect. In another word, the defect motion of the defect leaves a trace on the network structure and so that the defect's walk is far from random. This memory effect restricts defect's walk more as the average number of virtual HBs at a vertex is lowered. If there are only two virtual HBs at a vertex, a single defect cannot pass the vertex and is sometimes confined in a small region of the network, as easily proven. Such a property of defects restricts the propagation of HBR in the structured water.

TABLE VI. The probabilities, P_a, of disconnecting a hydrogen bond (HB) under various states of the terminal vertices, extracted from MD data at 220 K. The terminal vertices are two water molecules linked by the HB. The state of the terminal vertices is specified by the numbers of HEs attached to both terminal vertices, $\vec{z}_{\mathrm{HB}}$ (the number of the donating HBs) and $\overleftarrow{z}_{\mathrm{HB}}$ (the number of the accepting HBs).

$\vec{z}_{\mathrm{HB}}$	$\overleftarrow{z}_{\mathrm{HB}}$	P_a
1	1	0.098
1	2	0.117
1	3	0.352
2	1	0.083
2	2	0.100
2	3	0.294
3	1	0.226
3	2	0.294
3	3	0.727

V. LATTICE MODEL

Based on the decomposition scheme of the HBN graph and the HB state transition probabilities extracted from the trajectory calculations shown in the previous section, we are now ready to construct the lattice models of the HBN rearrangement dynamics in the supercooled water.

(1) Let us choose a simple (or body centered) cubic lattice. Each node of the lattice has 6(8) neighborhoods. and the lattice bonds represent the adjacency bonds of the water.
(2) Each bond has a directionality, an arrow, representing the incoming or outgoing hydrogen bond. Each node has 3(4) incoming and 3(4) outgoing arrows. we call these arrows as ''adjacency edges.''
(3) HEs are placed on the edges of the adjacency edge network. HEs occupy some fraction of the adjacency edges.

Then the next problem is how to propagate the network change. It is desirable to reproduce the network dynamics by a model with a minimum set of parameters. We choose two sets: The first is based on the state transition probabilities of the vertices shown in Fig. 2 and the other is based on that of the edges shown in Table VI. We call them method A and B, respectively. We separate the donating HBs and accepting HBs at individual nodes, i.e., using undirected graph representation, and impose the state transitions rule described in the previous section.

The following is the procedure to advance one simulation step.

Method A

(1) Choose randomly some adjacency edges and switch their HE occupancy from the occupied to vacant state, or conversely (we call this ''flip the edge'').
(2) Compare the modified network with original one. Repeat random HB flips until the transition probabilities P_{12}, P_{32}, P_{21}, P_{23} and $P_{22}^{\pm}$ of the whole change of the HB network coincide with a set of given values.

For actual application we have used $P_{12}=0.4$, $P_{32}=0.3$, $P_{21}=0.030$, $P_{23}=0.0041$, $P_{22}^{\pm}=0.05$ as transition probabilities; these probabilities are a little smaller than those values listed in Fig. 2, because this procedure becomes very time consuming as these probabilities get larger. Each simulation step contains several thousands of edge flips, and we performed 4096 steps.

Method B

(1) Randomly choose one edge.
(2) Count the number of HEs attached to each end vertices of the chosen edge.
   (a) If the chosen edge is not occupied:
      (i) If both end vertices are $\ominus$ defects, flip the edge with probability p.
      (ii) If one end vertex is $\ominus$ defect, flip the edge with probability q.
      (iii) If both are not $\ominus$ defects, flip the edge with probability r.
   (b) If the chosen edge is occupied:
      (i) Both end vertices are $\oplus$ defects, flip the edge with probability p.
      (ii) If one end vertex is $\oplus$ defect, flip the edge with probability q.
      (iii) If both are not $\oplus$ defects, flip the edge with probability r.

   Where p, q and r are pair annihilation, propagation and pair creation probabilities, respectively.
(3) Repeat the above procedure n_n times, where n_n is the number of nodes in the lattice.

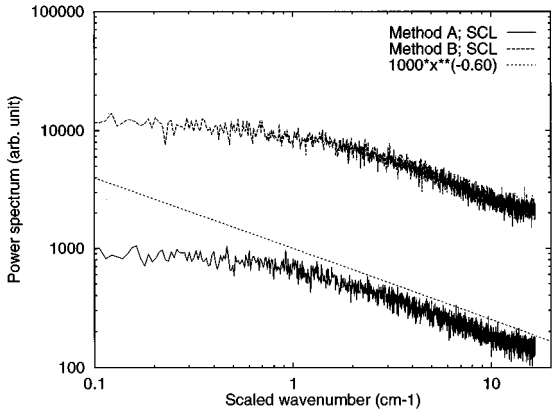

FIG. 5. Energy fluctuations in the model lattice systems are plotted in log–log scale. Upper lines are obtained by method B and lower by method A.

Here we assumed that the HB disconnecting probabilities p, q and r is equivalent to the HB connecting probabilities. For actual simulation, we have used 0.72, 0.29 and 0.10 for p, q and r, respectively.

By both methods, the average number of the HBs at an individual node is kept nearly to be 2+2. It should be noted here that some features of the real water are ignored in these lattice models. Water molecules can not translate, that is, there is no diffusion of the center of mass, and the lattice structure does no change. These assumptions will breakdown at high temperature and for long time dynamics of water.

To compare the magnitude of energy fluctuation, we divided the total system into sublattices, each of which includes $6\times6\times6=216$ nodes. We assume that the total potential energy of a sublattice is equal to the total number of HBs in the sublattice multiplied by a constant. Fourier transform of the potential energy fluctuation of sublattice thus obtained is plotted in the Fig. 5. Both methods reproduce the $1/f^{\alpha}$ spectra with $\alpha=0.6$ (f is the frequency), which is very close to the previous MD result with the exponent $\alpha=0.75$.[27] If HBs are randomly picked up and flipped, an energy fluctuation behaves as $1/f^2$.

The distribution of HB lifetime is also analyzed. It is found that the HB lifetime calculated by MD behaves as t^{α} in short time and decays exponentially in long time (not shown in figures). This behavior of HB lifetime was already pointed by Stanley *et al.*[28] As shown in Fig. 6, our lattice model well reproduces this HB life time distribution. Of course, if each HB flips with a single relaxation time, HB lifetime distribution must be exponential in all time region.

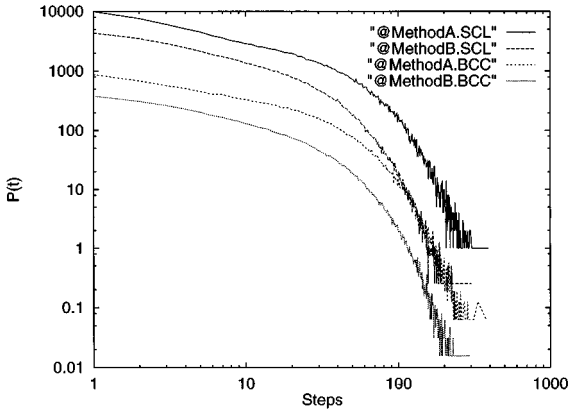

FIG. 6. HB lifetime distribution obtained for the models under various setting. From top: Result by method A with simple cubic lattice (SCL); method B with SCL; method A with body centered cubic lattice (BCC); method B with BCC. Vertical axis is in arbitrary unit.

In order to make a further analysis, we define the heterogeneity index for HBR. The frequencies of HBRs at nodes during n steps are counted and then averaged over the nodes. The average frequency in n steps is expressed by $\bar{m}_n$ and its spatial standard deviation by σ_n. The heterogeneity index is defined as

$$H_n=\frac{\sigma_n}{\bar{m}_n}. \tag{6}$$

$\bar{m}_n$ is expected to grow proportional to n. If the HBRs are homogeneous process, σ_n is proportional to $n^{1/2}$ and thus H_n decays with $n^{-1/2}$. If HBR are heterogeneous, the decay is slower than $n^{-1/2}$ as shown in the appendix. The heterogeneity index obtained by MD calculations is plotted against time in the Fig. 7(a). At high temperatures (260–300 K), the heterogeneity index initially decays slower than the homogeneous case, with the exponent of $\alpha<0.5$, but turns to be homogeneous for the time longer than 10 ps. At lower temperatures (200–220 K), the index has three slops. The curve decays slowly in the middle time domain, meaning that there is very long-lived heterogeneity. The heterogeneity index is also calculated for a sublattice with $6\times6\times6$ nodes in the lattice model, and is shown in the Fig. 7(b). Our models can reproduce the gentle slope as the MD curve in short time, $\alpha<0.5$, indicating the temporal correlation of HBs is described by our models. They cannot, however, reproduce the decay in long time dynamics, because translational motions, which causes large scale structural rearrangements of the HB network, are missing in the lattice models.

VI. CONCLUSION

We have analyzed the HBR dynamics by performing MD calculations and constructing the lattice model. The simple lattice model based on state transition diagram was shown to well reproduce all of the HB lifetime, the HBR pattern (in Hamming matrix) and the energy fluctuation, obtained from MD calculation of the supercooled water. Change of the propagation rule or of the lattice structure is expected not to make qualitative difference of the results. The properties found in the present system are expected to be found in many other systems whose dynamics is coupled to defects as in spinglass.

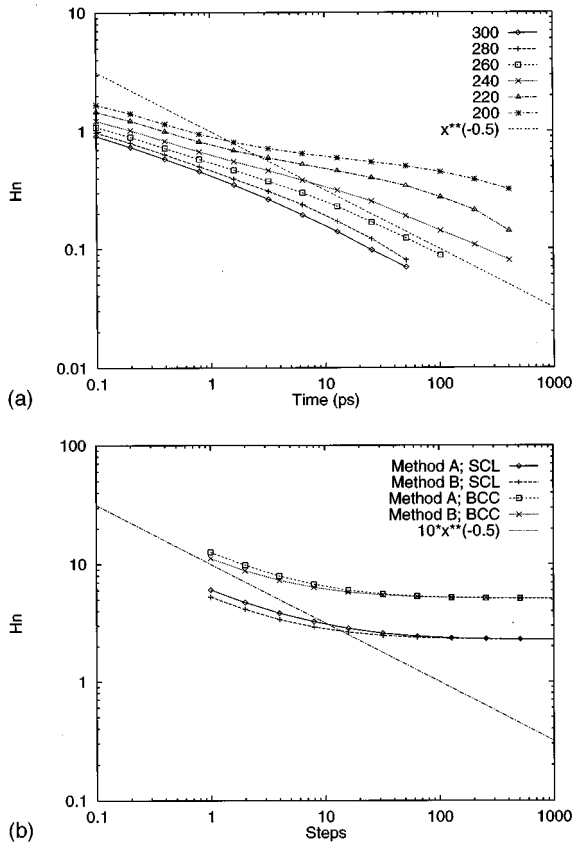

FIG. 7. The heterogeneity index defined in Eq. (6). (a) MD results; (b) lattice model. Straight dotted lines indicate $n^{-1/2}$ ($t^{-1/2}$) for an eye guide.

The analysis of the heterogeneity index indicated that HBRs are very heterogeneous. HBR was shown to be the motions of defects. Defect walks along the undirected graph, which is reduced from the three-dimensionally percolated directed graph. Even when the directed graph is constructed homogeneously and well percolated, the spatial edge (i.e., HB) connection among vertices in the undirected graph can be very heterogeneous. The motion of defects on the undirected graph is thus inhomogenized by the global network topology. Moreover, that the traces of the defect movements on the hydrogen bond network remain for a considerable time, inevitably localize HBR. When defects exist at some locations of the network, they rearrange HB connections in that local area (i.e., a subsystem of water). After defects leave that area, the local network is rarely rearranged. A subsystem, therefore, exhibits the energy fluctuation of $1/f^{\alpha}$ type, and yields domain structures in the distance matrix.[1,27]

These observations lead the conclusion that the existence of the defects and the network topology produce the spontaneous spatiotemporal fluctuation of HBR. The hydrogen bond network consequently becomes heterogeneous. The heterogeneity of the hydrogen bond network is thus not the origin of the heterogeneous HBR, but the result from the latter.

The picture presented in this work is valid only for the short-time dynamics of the supercooled water. Large displacements of molecules, which rearrange the topology of adjacency bonds (i.e., reconstruct the lattice) are missing in our model. These large displacements make HBR more homogeneous, resulting to the $t^{-1/2}$ slope of the heterogeneity index for very long time dynamics, as seen in Fig. 7. As the temperature becomes lower, however, correlated HBR becomes dominant. The heterogeneity index curve indicates that heterogenization contends with homogenization below 240 K.

It was found that there exist localized collective motions, involving large network rearrangement, in the liquid water even at room temperature.[1] In the current model, however, such collective motions can not be treated because our present model only deals with adjacent correlations. It is important to construct the models which are applicable in all temperature range.

ACKNOWLEDGMENTS

M. M. thanks to Professor M. Sasai for fruitful discussions and suggestions. This work is partially supported by the Grant-in-Aid for Scientific Research on Priority Areas of ''Chemical Reaction Theory,'' ''Photo Reaction Dynamics,'' ''Chemistry of Manybody Systems'' and ''Complex Fluids.''

APPENDIX: HETEROGENEITY INDEX

The heterogeneity index of random events occur on the network is calculated as follows. Suppose there are N bonds in the system. The ith event occurs at a randomly chosen bond. It is convenient to define the variable $x_i(a)$, which is 1 if an event occurs at the bond a at ith trial.

After n trials, average occurrence of events at a bond is simply denoted as

$$\bar{m}_n(a)=\sum_{i=1}^{n} x_i(a)=\frac{n}{N}. \tag{A1}$$

Spatial fluctuation of the occurrence of events is evaluated by the dispersion as

$$\begin{aligned}
\sigma_n^2 &= \frac{1}{N}\sum_{a=1}^{N}\left(\sum_{i=1}^{n} x_i(a)-\frac{n}{N}\right)^2,\\
&= \left\langle\left(\sum_{i=1}^{n}\left(x_i(a)-\frac{1}{N}\right)\right)^2\right\rangle,\\
&= \left\langle\sum_{i=1}^{n}\left(x_i(a)-\frac{1}{N}\right)\cdot\sum_{j=1}^{n}\left(x_j(a)-\frac{1}{N}\right)\right\rangle,\\
&= \left\langle\sum_{i=1}^{n}\left(x_i(a)-\frac{1}{N}\right)^2+2\sum_{i=1}^{n}\sum_{i\neq j}^{n}\left(x_i(a)\right.\right.\\
&\qquad \left.\left.-\frac{1}{N}\right)\left(x_j(a)-\frac{1}{N}\right)\right\rangle,
\end{aligned}$$

where the second term of the last formula becomes 0 because each event is independent.

$$\begin{aligned}
&= \left\langle\sum_{i=1}^{n}\left(x_i(a)^2-2\cdot x_i(a)\cdot\frac{1}{N}+\frac{1}{N^2}\right)\right\rangle,\\
&= \left\langle\frac{n}{N}-2\cdot\frac{n}{N}\cdot\frac{1}{N}+\frac{n}{N^2}\right\rangle,\\
&= n\cdot\frac{1}{N}\left(1-\frac{1}{N}\right).
\end{aligned}$$

It comes that $\sigma_n/\bar{m}_n$ is proportional to time $n^{-1/2}$. While if the events does not occur fairly in space, $\bar{m}_n(a)$ differs for each bond and that $\sigma_n/\bar{m}_n$ converge to nonzero value after a long time.

[1] H. Tanaka and I. Ohmine, J. Chem. Phys. **91**, 6318 (1989).
[2] I. Ohmine and H. Tanaka, Chem. Rev. **93**, 2545 (1993).
[3] I. Ohmine, J. Phys. Chem. **99**, 6767 (1995).
[4] M. Cho, G. R. Fleming, S. Saito, I. Ohmine, and R. M. Stratt, J. Chem. Phys. **100**, 6672 (1994).
[5] P. D. Flemming III and J. H. Gibbs, J. Stat. Phys. **10**, 157 (1974); C.-K. Hu, J. Phys. A **16**, L321 (1983); G. M. Bell and D. A. Lavis, *ibid*. **3**, 427 (1970); G. M. Bell, J. Phys. C **5**, 889 (1972); G. M. Bell and D. W. Salt, Trans. Faraday Soc. 2, **72**, 76 (1976); P. H. E. Meijer, R. Kikuchi, and P. Papon, Physica A **109**, 365 (1981); P. H. E. Meijer, R. Kikuchi, and Eddy van Royen, *ibid*. **115**, 124 (1982); H. E. Stanley and J. Teixeira, J. Chem. Phys. **73**, 3404 (1980).
[6] M. Sasai, Bull. Chem. Soc. Jpn. **66**, 3362 (1993).
[7] G. W. Robinson, J. Lee, K. G. Casey, and D. Statman, Chem. Phys. Lett. **123**, 483 (1986).
[8] R. L. Blumberg, H. E. Stanley, A. Geiger, and P. Mausbach, J. Chem. Phys. **80**, 5230 (1984).
[9] M. Sasai, J. Chem. Phys. **93**, 7329 (1990).
[10] S. Sastry, F. Sciortino, and H. E. Stanley, J. Chem. Phys. **98**, 9863 (1993).
[11] D. E. Hare and C. M. Sorensen, J. Chem. Phys. **93**, 25 (1990).
[12] R. Lamanna, M. Delmelle, and S. Cannistraro, Phys. Rev. E **49**, 2841 (1994).
[13] J. L. Green, A. R. Lacey, and M. G. Sceat, J. Phys. Chem. **90**, 3958 (1986).
[14] W. Nadler and Thomas Krausche, Phys. Rev. A **44**, R7888 (1991).
[15] G. P. Johari, A. Hallbrucker, and E. Mayer, J. Chem. Phys. **92**, 6742 (1990).
[16] C. A. Angell, J. Phys. Chem. **97**, 6339 (1993).
[17] H. E. Stanley, C. A. Angell, U. Essmann, M. Hemmati, P. H. Poole, and F. Sciortino, Physica A **205**, 122 (1994).
[18] P. H. Poole, U. Essmann, F. Sciortino, and H. E. Stanley, Phys. Rev. E **48**, 3799, 4605 (1993); H. E. Stanley, C. A. Angell, U. Essmann, M. Hemmati, P. H. Poole, and F. Sciortino, Physica A **205**, 122 (1993).
[19] F. Sciortino, A. Geiger, and H. E. Stanley, Nature (London) **354**, 218 (1991).
[20] F. Sciortino, A. Geiger, and H. E. Stanley, J. Chem. Phys. **96**, 3857 (1992).
[21] F. H. Stillinger, Science **209**, 451 (1980).
[22] R. J. Speedy, J. Phys. Chem. **88**, 3364 (1984).
[23] H. C. Andersen, J. Chem. Phys. **72**, 2384 (1980).
[24] S. Nosé, Mol. Phys. **52**, 255 (1984).
[25] W. L. Jorgensen, J. Chandrasekhar, J. D. Madura, R. W. Impey, and M. L. Klein, J. Chem. Phys. **79**, 926 (1983).
[26] G. Ruocco, M. Sampoli, A. Torcini, and R. Vallauri, J. Chem. Phys. **99**, 8095 (1993).
[27] M. Sasai, I. Ohmine, and R. Ramaswamy, J. Chem. Phys. **96**, 3045 (92).
[28] F. Sciortino, P. H. Poole, H. E. Stanley, and S. Havlin, Phys. Rev. Lett. **64**, 1686 (1990).